

# Assessment of Land Surface Subsidence Due to Underground Metal Mining Using Integrated Spaceborne Repeat-Pass Differential Interferometric Synthetic Aperture Radar (DInSAR) Technique and Ground Based Observations

Md Soyeb Alam<sup>1</sup> · Dheeraj Kumar<sup>1</sup> · R. S. Chatterjee<sup>2</sup> · Vijay Upreti<sup>1</sup>

Received: 5 September 2016 / Accepted: 16 July 2018 / Published online: 23 July 2018  
© Indian Society of Remote Sensing 2018

## Abstract

Differential interferometric synthetic aperture radar (DInSAR) is a novel remote sensing technique to measure earth surface deformation. It is capable of obtaining dense information related to the deformation of a large area efficiently, economically and effectively. Therefore, DInSAR is a promising technology for monitoring the earth surface deformation related to some natural hazardous events, such as earthquake, volcano eruption, land subsidence, landslide. In present study, Conventional DInSAR technique have been applied to a mineral rich zone, coming under the Khetri copper belt, a part of Northern Aravali range of hillocks in India, predominant with mining activities since late 1960's to address the possibility of deformation phenomena due to hard rock underground metal mining. Four interferometric SAR data sets of Radarsat-2 was used for the study area to address the subsidence/uplift phenomena. Further, results obtained from conventional DInSAR technique using Radarsat-2 data sets compared with results obtained from ground based observation technique for its validity. In both the techniques, deformation results obtained in terms of average subsidence rate in mm (quarterly basis) of points under study within mining zone of Mine-A has well agreed to each other. Further, it has been observed that average subsidence rate in mm (quarterly basis) obtained from space based observation and ground based observation are 5.6 and 6.67, respectively over the points under study in mining zone of Mine-A.

**Keywords** Subsidence · Underground metal mining · Conventional DInSAR · DEM · GCP

## Introduction

Subsidence is one of the most noticeable environmental impacts associated with mining. Mine subsidence is a movement of the surface in the form of small scale collapses such as, sinkholes or troughs on the surface and regional settlements as a result of settlement of the overburden due to disintegration or failure of underground mine workings. Subsidence can have severe economical, technical, social, and environmental impacts. The most

common impacts of mine subsidence are observed on surface structures, bridges, buildings, services and communications lines, and agricultural land through the disruption of drainage patterns and variations of gradient. The extent of potential impacts of subsidence depends on the type of mining method, geology of the deposit and the overburden, attitude of the mineral deposits, and mitigation measures. Generating appropriate mitigation measures necessitates continuous monitoring and investigation of the mine area and its surroundings. In this sense, remote sensing can provide an effective tool in measuring and interpreting subsidence quickly, accurately, and simply.

Monitoring of mining induced subsidence is of vital importance to mining professionals and community for taking appropriate mitigation measures to avoid and control subsidence. Among the various space-borne techniques available till date for measuring ground deformation,

---

✉ Md Soyeb Alam  
multisoyeb2004@gmail.com

<sup>1</sup> Department of Mining Engineering, Indian Institute of Technology (Indian School of Mines), Dhanbad, India

<sup>2</sup> Geosciences and Disaster Management Studies, Indian Institute of Remote Sensing, ISRO, Dehradun, India

D-InSAR technique is considered to be the most efficient way for measuring spatially-continuous ground deformation with higher precision. The precision and feasibility of D-InSAR technique is largely controlled by the quality of InSAR data pairs, in terms of baseline and wavelength of the SAR signal.

Recent developments in satellite geodesy techniques by using spaceborne D-InSAR, introduced a new tool to detect and measure subtle vertical displacements (cm to sub-centimeter level).

DInSAR technique developed in different stages e.g. Conventional DInSAR, First generation Time-series InSAR (Advanced DInSAR) and second generation time-series InSAR (JSInSAR/DSInSAR).

Most of the researchers till the development of advanced DInSAR and or Joint scatterer InSAR have used conventional DInSAR technique for monitoring long-term land subsidence phenomenon (Zebker and Goldstein 1986; Zebker and Rosen 1994; Gabriel et al. 1989; Goldstein 1995; Rosen et al. 1996; Galloway et al. 1998; Massonnet and Feigl 1993, 1996, 1997; Strozzi et al. 2001; Amelung et al. 1999, 2000; Usai 2001; Colesanti et al. 2002, 2003; Hanssen and Usai 1997; Hanssen et al. 1999, Hanssen 2001; Fruneau and Sarti 2000; Lanari et al. 2007; Chatterjee 2006, Raucoules et al. 2009). However, conventional DinSAR technique having its own limitations in terms of very small spatial baseline (< 200 m), baseline dependent accuracy of external DEM, no reduction of atmospheric phase etc. (Ferretti et al. 2000).

To overcome the limitations associated with conventional DInSAR technique, first generation time series InSAR (Advanced DInSAR) technique was introduced by Ferretti et al. 2000, 2001. Subsequently many researchers have worked on advanced DInSAR technique and developed different approaches (Berardino et al. 2002; Hooper et al. 2004; Hooper 2008; Mora et al. 2003; Schmidt and Bürgmann 2003; Werner et al. 2003; Duro et al. 2003; Crosetto et al. 2005, 2008; Kampes 2006; Costantini et al. 2008; Van Leijen and Hanssen 2007; López-Quiroz et al. 2009). However, advanced DInSAR technique having its own limitations in terms of point based analysis, compelling to study only permanent scatterer causes less spatial coverage of study area. Although, this technique helps in reduction of atmospheric phase, besides it, very small baseline and high accuracy of external DEM are not the criteria (Ferretti et al. 2000).

Keeping in view to overcome the limitations associated with advanced DInSAR technique, Second generation time series InSAR technique (SqueeSAR) was introduced by Ferretti et al. (2011). Subsequently many researchers worked on second generation time series InSAR and developed different approaches (Perissin and Wang 2012; Hetland et al. 2012; Goel and Adam 2014; Lv et al. 2014;

Devanthery et al. 2014) to identify the areas affected by land subsidence and an attempt was made to measure precisely the rate of land subsidence phenomenon in order to prepare a spatially continuous land subsidence map. This technique is also known as Joint scatterer technique or Distributed scatterer technique. In this technique/approach algorithm was developed to include the distributed scatterers from less coherent area to increase the spatial density of measurement points in the study area this particular algorithm/approach is based on statistically homogeneity test.

In Present study, Conventional DInSAR technique is applied to understand the subsidence phenomena in the study area which belongs to one of the rich copper mining activity zone keeping in view of non-availability of stack of InSAR data sets.

## Objectives of Present Study

The main objectives of the present research work are as follows:

1. Detection and assessment of open Stopping induced land surface subsidence in hard rock metal mine area using spaceborne repeat-pass differential interferometric synthetic aperture radar (DInSAR) Technique.
2. Quantitative validation of results obtained from space based observation technique by ground based observations.

## Salient Features of Study Area

### Geographical Information

The Khetri Copper Complex has two underground working mines namely Mine-A and Mine-B. The Mining Lease area is situated at the northern tip of the Khetri Copper Belt. It covers an area of 162.23 hectare. The area falls in the Survey of India Topo sheet No. 44/P16. Main hill ranges in the lease hold area strikes NNE-SSW located at the western side of half of the area. The hill ranges contain the host rock of copper mineralization. The western slope of the hill is steep while the eastern slope is relatively gentle. The lease-hold area is marked on the Survey of India Toposheet no.44P/16 in 1:50000 scale. The Mine A and Mine B is well connected by metalled road. The nearest railway station is Nizampur on Rewari-Jaipur section (North Western Railway) and another is Chirawa (30 km) on Loharu-Jaipur section (North Western Railway). The geographical location of study area is (Latitude N 28°00'46" to N 28°05'50"

and Longitude E  $75^{\circ}45'32''$  to E  $75^{\circ}49'53''$ . Location map of study area is shown in Fig. 1.

## Topography

The topographical analysis of Mine-A reveals that the mineralized hill ridge of the Mine-Block which is about 2.5 km N  $15^{\circ}$ W of Bhopalgarh Fort and about 2 km NW of Khetri town, stretches about 640 ms in N  $18^{\circ}$ E direction which is almost co-incident with the axis of the hill N  $16^{\circ}$ E. The knife-edge exposure of hard and tough massive peak-quartzite attains a height of 670 M above MSL. The strike directions, corresponding to the western slopes and eastern are North and N  $34^{\circ}$ E whereas the inclinations are  $36^{\circ}$  and  $32^{\circ}$  respectively i.e. in general western slope is steeper, more rugged and difficult to traverse than the eastern slope. The region is covered by thorny bushes mainly kickers, other jungle trees are also not uncommon. The eastern valley having the lowest level of 422 M above MSL rises gradually till the base of the hill while beyond this the rise is fairly steep. The western foot hill, the lowest level at the base is 460 M above MSL, is joined with the

number of hillocks covered with the sand-dunes. The entire stretch of 2 km in the west, from foot hill to Kharkhara seasonal river is covered with the sand-dunes. The general inflow of water is both on east and west slopes of the main hill range, but due to vast coverage with sand –dunes and sandy soil on the west, the water gets absorbed whereas on the eastern side this in-flow of water during short rainy days in the season causes flood. The general trend of the stream at the eastern valley level is towards southeast. Whereas Mine-B area forms a part of northern extremity of Aravali range of hills. There are three NE-SW striking ranges separated by sandy plains within the lease boundary. Towards west, falls the eastern foot-hill of Makro Hill range. The central hill range contains copper mineralization. This hill range is separated by Kharkhara Valley from Makro Hills. On further eastern side, there is magnetite-quartzite hill of moderate height/elevation separated by the valley where different plants, stores, administrative building etc. are located. The slopes of the hills are very steep with little soil cover. Whereas the southern part of Mine-A lease boundary is a hilly terrain, the northern part is soil covered plain area. The highest point of the area is 555 m

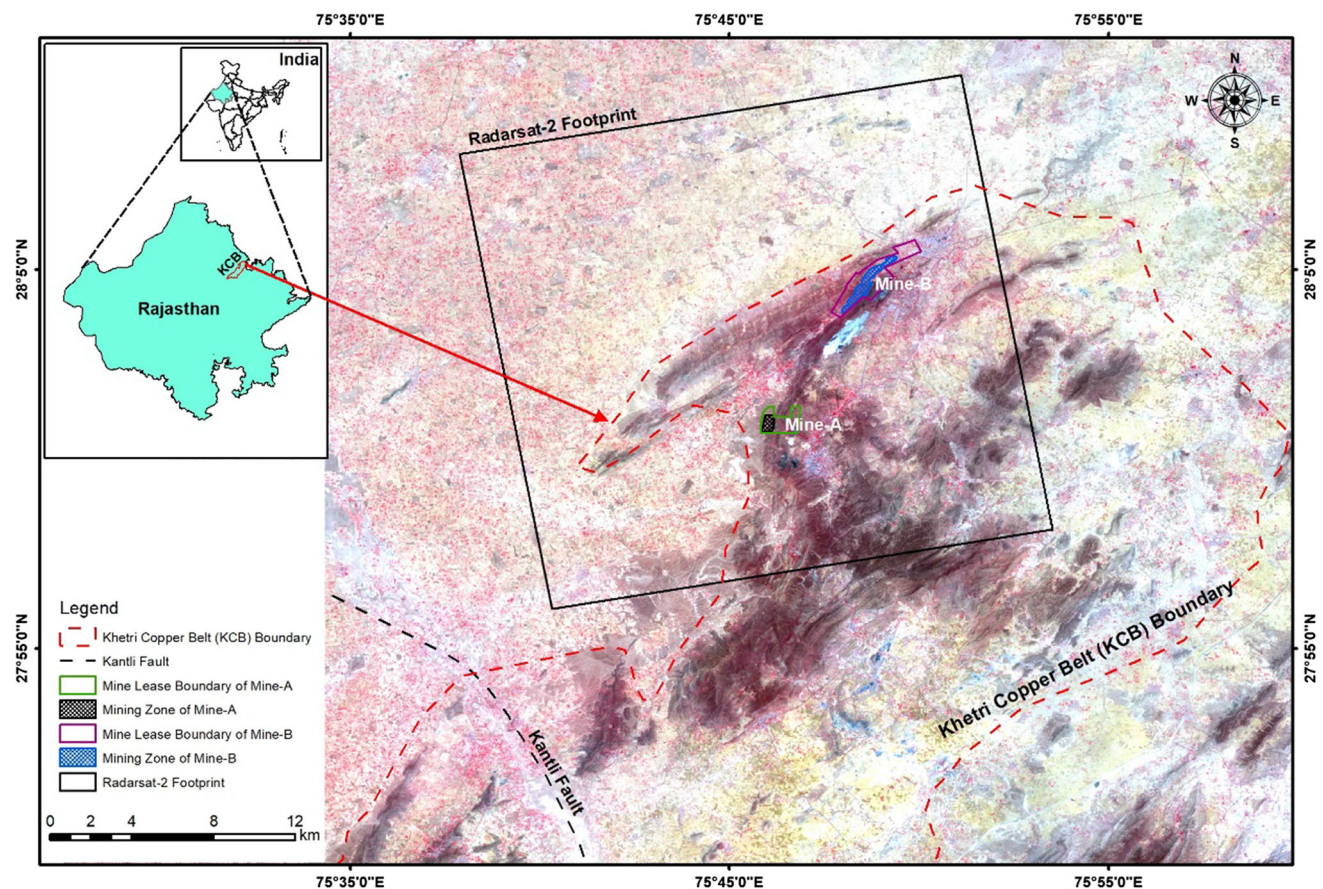


**Fig. 1** Location map of the copper-mining areas (Mine-A and Mine-B) in Khetri Copper Belt (KCB), Rajasthan, India and the image coverage of Radarsat-2. The background map is optical satellite imagery (LISS IV) of KCB



above mean sea level and the valley level is around 350 m above mean sea level. There are two seasonal nallas, namely Kharkhara in the west and Sukhnadi on the eastern side of the lease boundary of Mine-A. Natural flow of water in the drainage system of this area has a trend towards NE.

## Geology

The rocks in the Khetri district belong to the Delhi Supergroup of Precambrian age, which is sub-divided into the Alwar and Ajabgarh Groups. The older Alwar rocks are derived from predominantly arenaceous sediments while the younger Ajabgarh rocks were originally more argillaceous; the transition between the two is gradational. All these formations are metamorphosed to quartzites, schists and phyllites. Some intrusive dolerite dykes are present and veins of quartz and carbonate are common. The general strike of the formation is NNE-SSW with steep to gentle dips towards the WNW. The economic mineralization, which gives rise to the ore bodies, is mainly localized in the upper parts of the amphibole-chlorite-quartzite and garnet-amphibole-chlorite-quartzite/schist. The mineralization occurs in the form of veins, veinlets, stringers and disseminations (rarely massive), oriented in general parallel to the foliation plane. In Mine-B, there are two distinct ore lodes, namely Madhan (or footwall) lode and the Kudhan (or hanging wall) lode. The Madhan lode is fairly persistent, containing a number of ore lenses. The Kudhan lode, on the other hand, is narrower, poorer in copper, and the lenses are less persistent. It is well formed in the central part of the mine. Whereas, in the Mine-A, there are three distinct lode systems: Lode (south lode), Lode II (north lode) and Lode III (east or footwall lode). Lode I and III are persistent but Lode II is not persistent in depth.

## Relevant Details of Mine Workings

Mine-A has been developed over a strike length of 700 m and has eight levels at vertical interval of 60 m viz. 424, 364, 306, 246, 184, 124, 64 and 0 m reduced levels (m RL). The numbers indicate the height of the respective level above Mean Sea Level. The upper four levels viz. 424, 364, 306 and 246 m RL are exhausted and topmost three levels are isolated from rest of the mine. Production is going on in two levels namely 184, 124 m RL and Mine development is going on at four levels 184, 124, 64 and 0 m RL. Stope development in strike extension at 306 and 246 m RL is also being planned to increase stope availability. Whereas Mine-B has been developed over a strike length of 3425 m and has eight levels at vertical interval of 60 m viz. 421, 350, 300, 240, 180, 120, 60 and 0 m reduced levels (m RL). The numbers indicate the height of the respective level above Mean Sea Level. The upper four levels viz. 421, 350, 300 and 240 m RL are exhausted and topmost three levels are isolated from rest of the mine. Production is going on in three levels namely 180, 120 and 60 ML and Mine development is going on at four levels 180, 120, 60 and 0 m RL. 2nd stage mine development below 0 m RL is under progress.

## Remote Sensing Data Sets Used

### Cartosat-1 Stereo Pair

Basic information of Cartosat-1 stereo pair data sets used for DEM generation is shown in Table 1.

### Radarsat-2

Basic information of Radarsat-2 (RS-2) InSAR data sets used for interferometry is listed in Table 2.

**Table 1** Basic information of Cartosat-1 stereo pair data sets used for DEM generation

Satellite image no.	Satellite/sensor/agency	Path/row	Date of pass	Resolution (along × across)
1	Cartosat-1/Pan_fore/NRSC	0518/268	13 June, 2010	2.5 m × 2.5 m
2	Cartosat-1/Pan_aft/NRSC	0518/268	13 June, 2010	2.5 m × 2.5 m

**Table 2** Basic information of Radarsat-2 InSAR data sets used for interferometry

Satellite image No.	Satellite/sensor/agency	Date of PASS	Resolution along	Resolution across	Off-nadir angle (°)
1	RS-2/SAR/CSA	Jan 25, 2016	2.8	1.6	43.7
2	RS-2/SAR/CSA	Feb 18, 2016	2.8	1.6	43.7
3	RS-2/SAR/CSA	March 13, 2016	2.8	1.6	43.7
4	RS-2/SAR/CSA	April 6, 2016	2.8	1.6	43.7

## Research Methodologies

Integrated approach has been adopted to address the land surface deformation due to hard rock underground metal mining using space based differential interferometric synthetic aperture radar (DInSAR) technique and ground based observations technique for the study area. Subsequently,

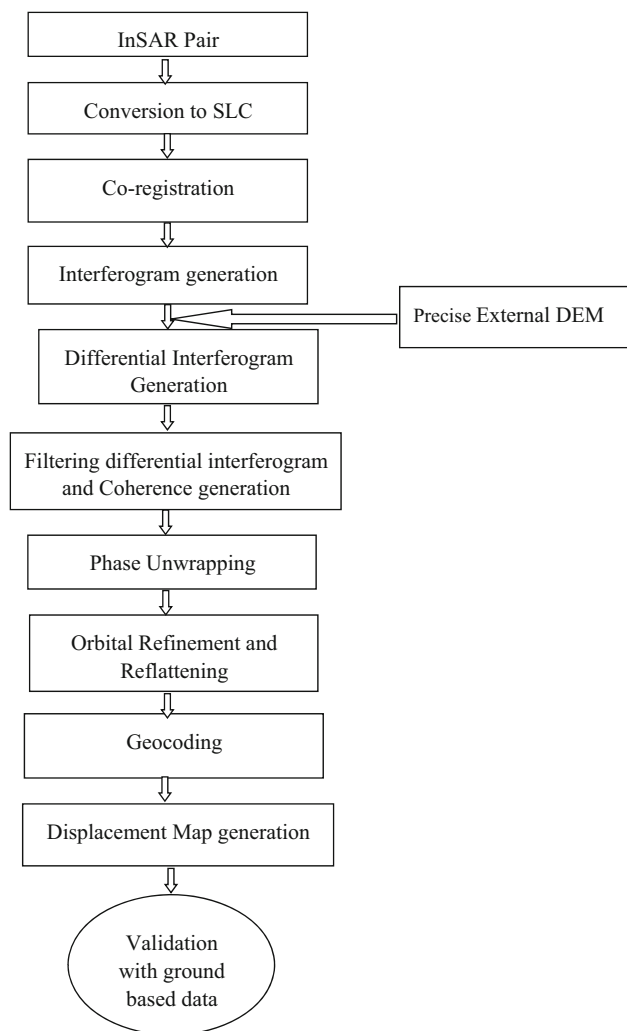


**Fig. 2** Research methodology for DInSAR processing and validation of result by ground based observations

Results obtained from space based technique compared with ground based observations technique. However, in present study Mine-A has been considered for validation of results obtained from space borne repeat-pass interferometry with ground based observations keeping in view of expected relatively higher subsidence rate. Research methodology for integrated approach shown in Fig. 2. Further, Mining zone of Mine-A of the study area splitted by taking transverse sections of 50 m interval based on the availability of points under study on the ground as shown in Fig. 7. Points were studied for its any possible movement at an interval of 25 m along the different transverse sections and used to validate the DInSAR results of corresponding points.

## Observations

### Baseline Estimation and Coherence Map Generation of Radarsat-2 InSAR Data Sets

To obtain information about the baseline values and other orbital parameters related to the input pair, baseline estimation is carried out. Baseline estimation of Radarsat-2 InSAR data sets is shown in Table 3. Further, filtered coherence maps of all the possible pairs are generated to know the phase quality of the interferometric data sets. Furthermore, for removing atmospheric phase from interferogram 1–4 (taken for the present study), common high coherence value points is selected with help of all possible coherence maps. Figure 3 shows coherence map of 1–4 interferometric data set showing the common high coherence value points (marked with red circles)

## Results and Discussion

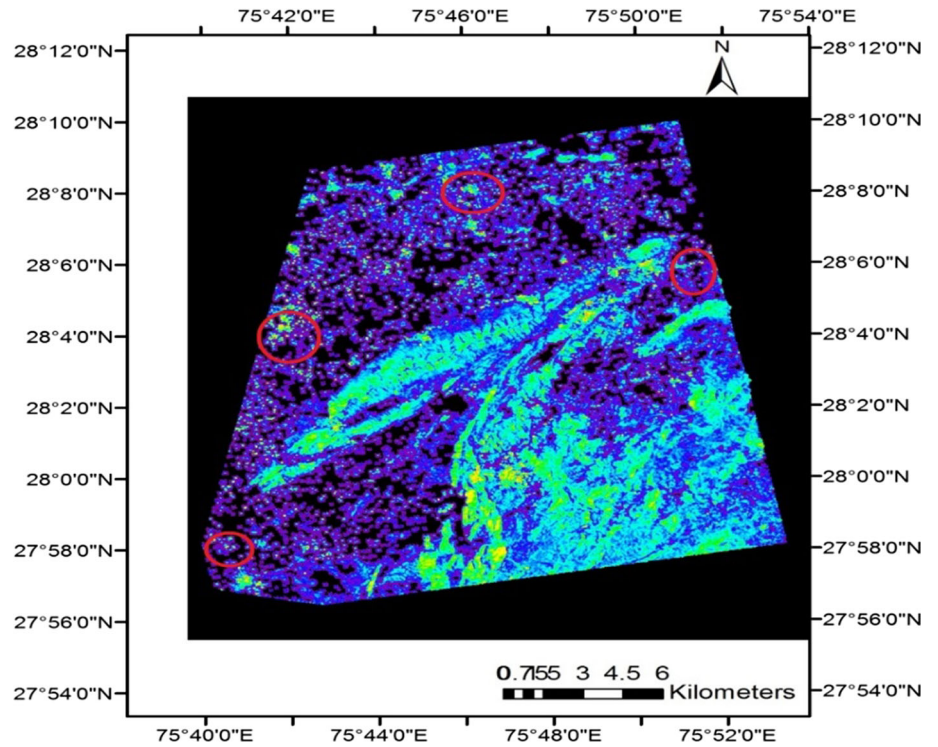
### Cartosat-1 DEM Generation and Validation

In DInSAR processing, baseline dependent DEM is required in order to eliminate the topographic phase. Normal baseline above 100 m particularly in the order of

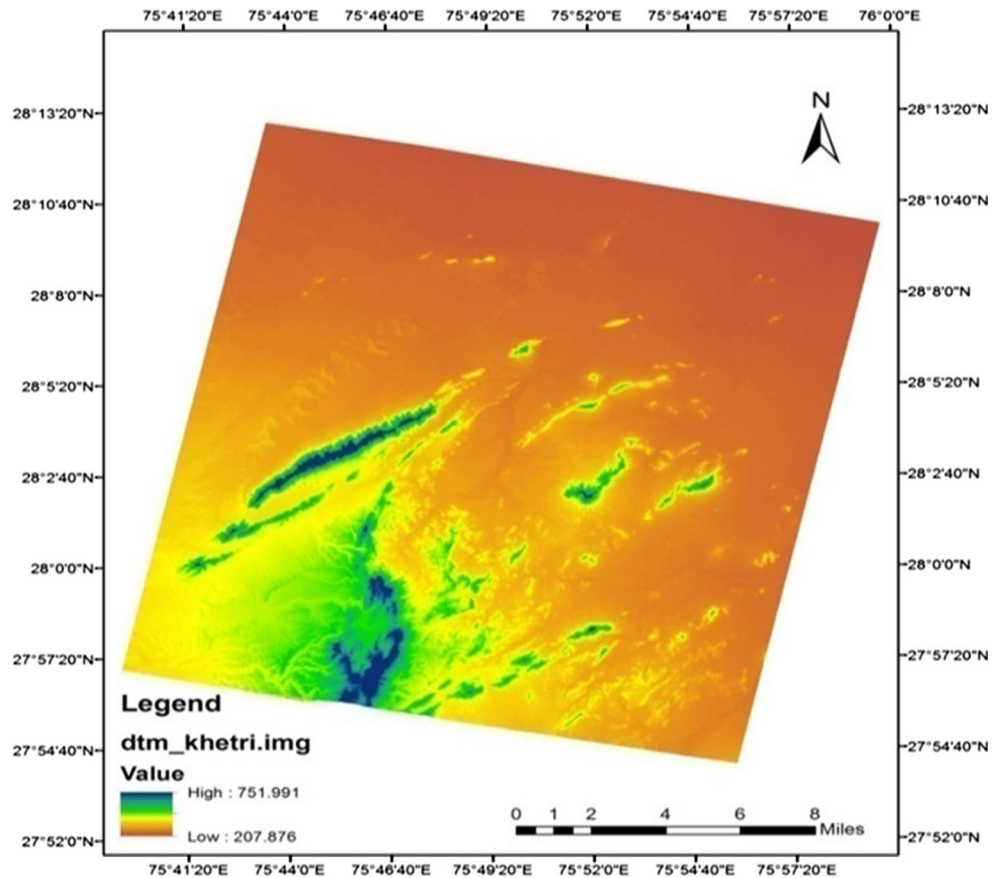
**Table 3** Baseline estimation of Radarsat-2 interferometric data sets

InSAR pair	Normal baseline (m)	Temporal baseline (days)	Range shift (pixel)	Azimuth shift (pixel)	Doppler Shift difference (Hz)
1–2	– 128.618	24	– 60.421	– 106.121	– 62.531
1–3	– 30.604	48	2.863	– 109.744	– 64.668
1–4	– 104.584	72	– 34.289	– 62.257	– 20.576
2–3	120.422	24	63.780	– 3.615	– 2.137
2–4	26.433	48	26.628	45.867	41.955
3–4	– 97.590	24	– 36.658	49.484	44.092

**Fig. 3** Coherence map of InSAR pair 1–4; red circles are indicating high coherence value Points used for removing atmospheric phase



**Fig. 4** DEM generated using GCPs (collected from Dual frequency GNSS)



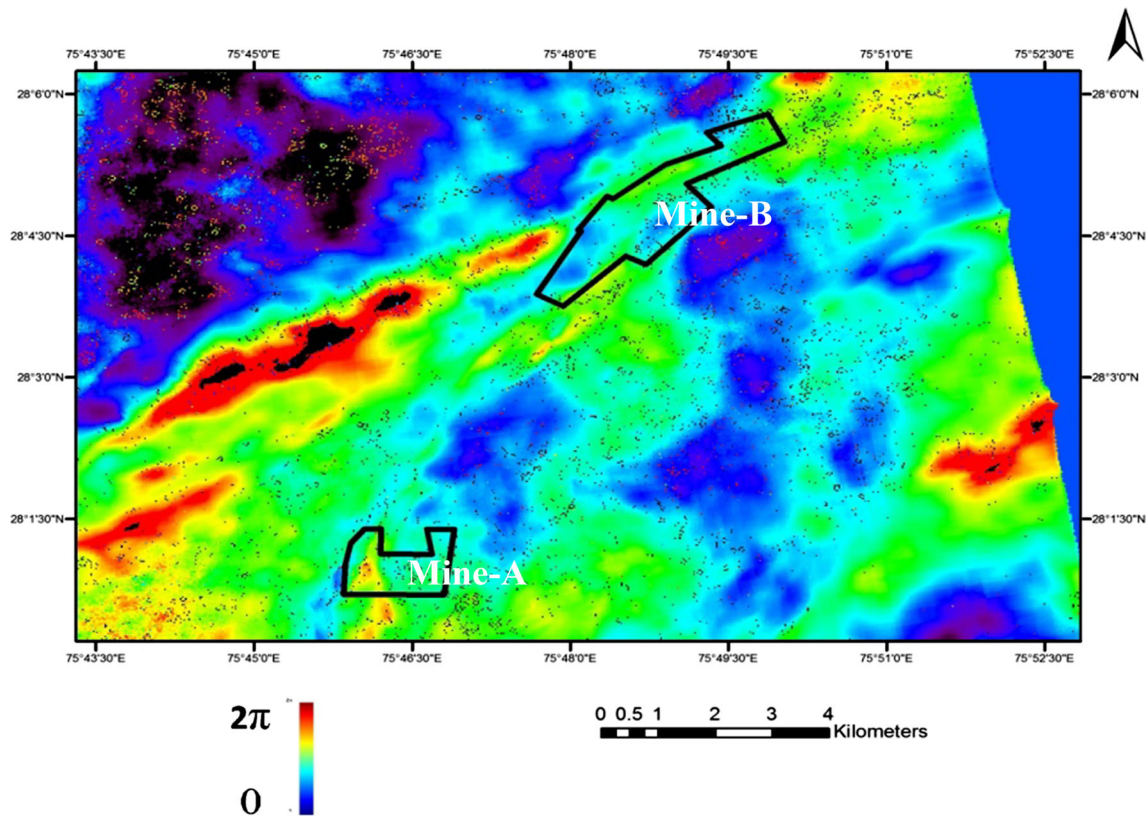


**Fig. 5** Filtered differential Interferogram of Interferometric SAR Pair 1–4 superimposed on mine lease boundary of Mine-A and Mine-B

200–250 m produces good topographic phase. Therefore, precise Cartosat-1 DEM was generated and validated. Figure 4 shows the DEM generated using GCPs Collected from dual frequency GNSS. The RMSE of 3 m (approx.) obtained between the differences of ellipsoidal height of Cartosat-1 DEM generated using GCPs Collected from dual frequency GNSS and test/check points.

### **DInSAR Derived Filtered Differential Interferogram Versus Underground Workings**

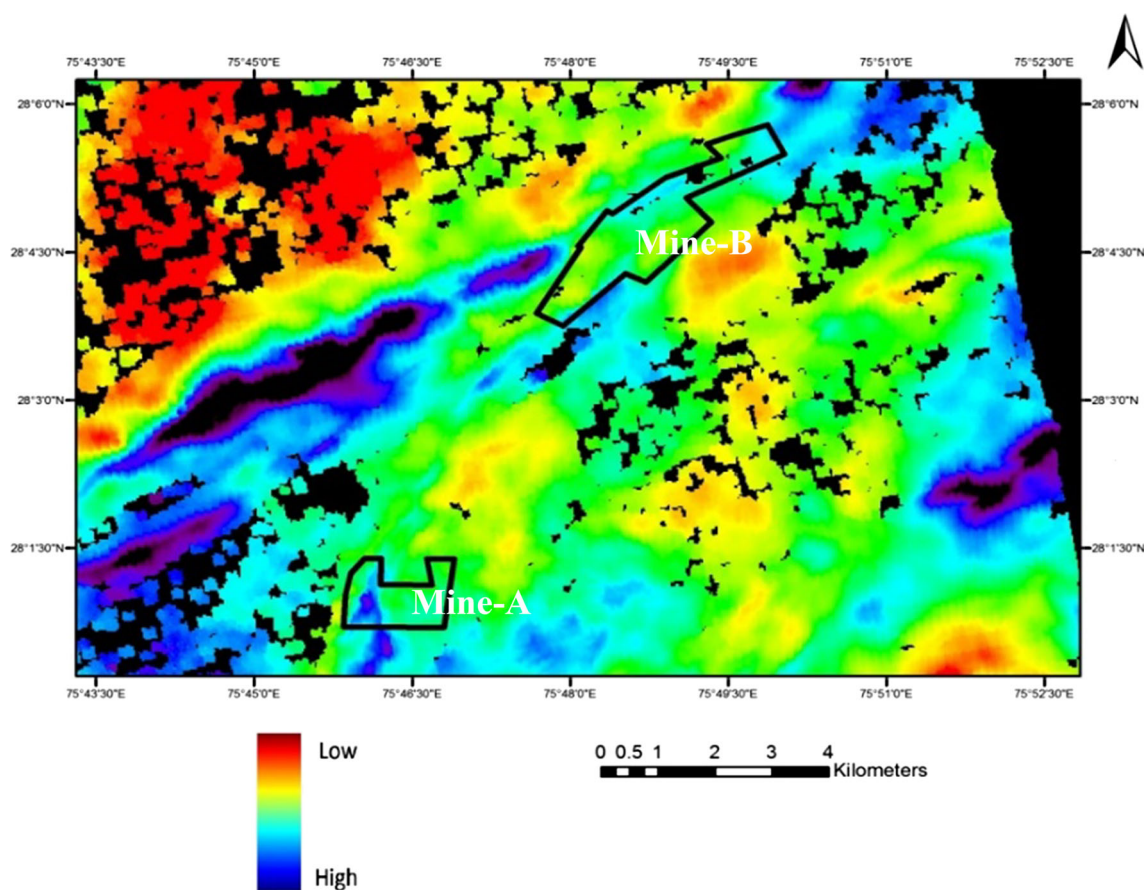
All possible filtered differential interferograms were generated. Differential interferogram generated using InSAR pair 1–4 was taken for the present study keeping in view of expected deformation rate in the study area (see Fig. 5). Figure 5 shows filtered differential interferograms superimposed on mine lease boundary of Mine-A and Mine-B.

Figure 5 shows that in mining zone of Mine-A, there is a development of concentric fringe which represents the mining subsidence trough.

### **DInSAR Derived Displacement Versus Underground Workings**

Displacement map was generated from the filtered differential interferogram 1–4 and subsequently superimposed on the mine lease boundary of Mine-A and Mine-B (see Fig. 6). From Fig. 6, it is quite evident that in mining zone of Mine-B relatively higher displacement exists. Further, displacement map is zoomed in and superimposed on underground workings and points under study in the vicinity of mining zone of Mine-A (see Fig. 7).





**Fig. 6** Displacement Map of Interferometric SAR Pair 1–4 superimposed on mine lease boundary of Mine-A and Mine-B

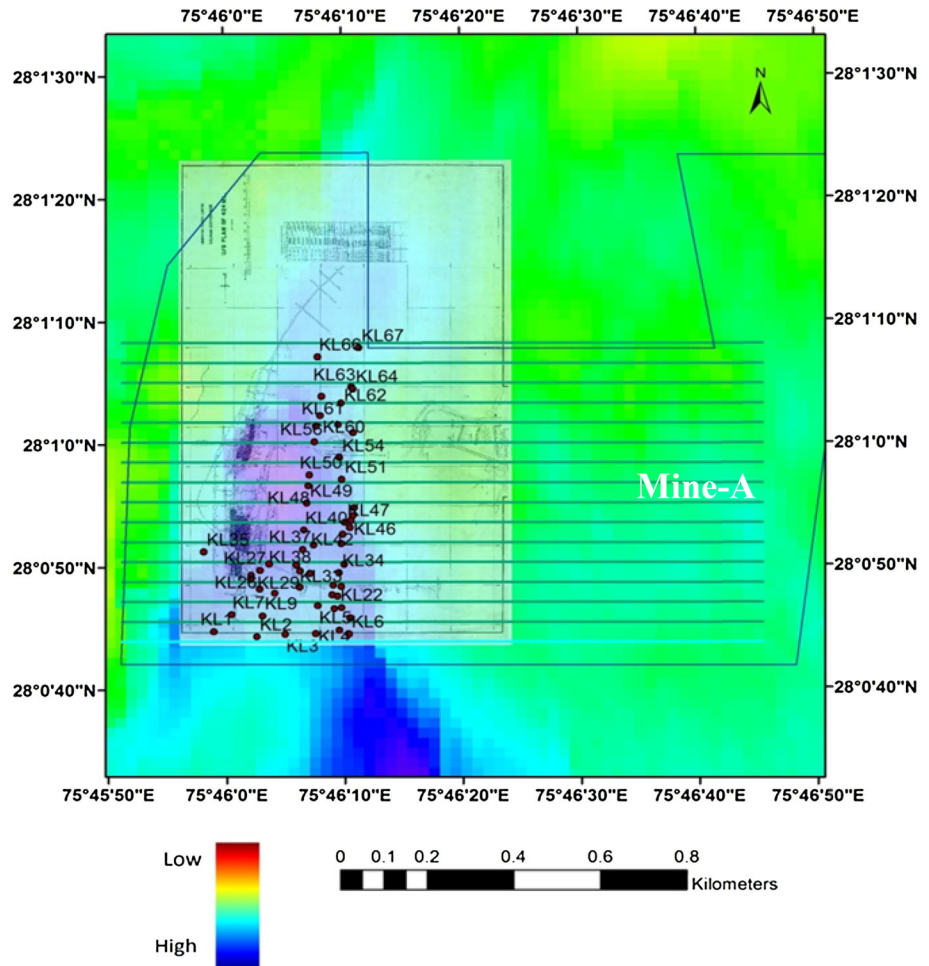
### Comparison of Subsidence Rate

Results in terms of subsidence rate obtained from space based observation has well agreed to the results obtained from ground based observation as shown in Figs. 8a–j and 9. Further, it has been observed that average subsidence rate in mm (quarterly basis) obtained from space based observation and ground based observation are 5.61 and 6.67, respectively over the points under study in mining zone of Mine-A. Result obtained from space based observation is not free from all the errors specially error due to temporal decorrelation. Attempts have been made to remove the atmospheric phase and phases due to sources of

decorrelation excluding temporal and spatial from the points under study within mine lease boundary by selecting high coherence value pixels outside the mine lease boundary from the coherence map. It has been found that the average coherence value of the points under study within mine lease boundary is 0.6. Average coherence value (0.6) indicates that points under study are not free from the errors due to the temporal and spatial decorrelation. Normal baseline (Table 3) of the used interferometric dataset (1–4) indicates that decorrelation due to spatial baseline is not significant hence; temporal decorrelation plays a vital role in the accuracy of the subsidence result obtained for the points under study.



**Fig. 7** Displacement Map of Mine-B superimposed on points under study along transverse sections and underground working



## Conclusions and Suggestions for Future Work

### Conclusions

- Results of average subsidence rate (in mm quarterly basis) obtained from space based observation and results obtained from ground based observation are 5.61 and 6.67, respectively over the points under study in mining zone of Mine-A and both the results have agreed well to each other.
- Subsidence value obtained from space based observation of points under study within mining zone of Mine-A is not completely free from phase noise

particularly due to the temporal decorrelation which governs the accuracy of conventional DInSAR

- Attempts have been taken to remove residual atmospheric phase from the points under study with the help of pixels having coherence value above 0.9

### Future Scope of Work

- Further well established approach to be taken in order to remove the residual atmospheric phase from the points under study.
- Second Generation Advanced DInSAR technique could be one of the tools for overcoming the

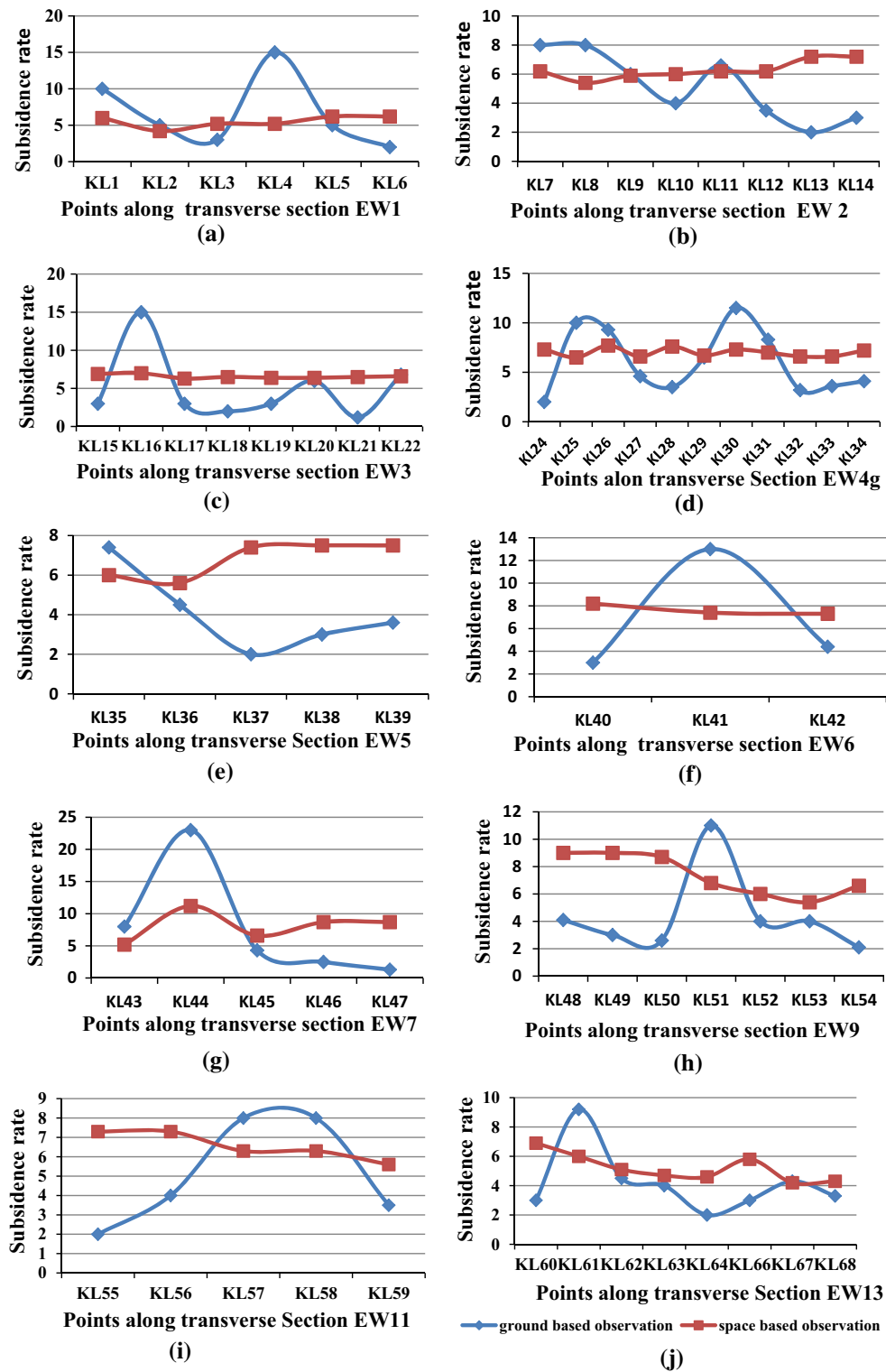
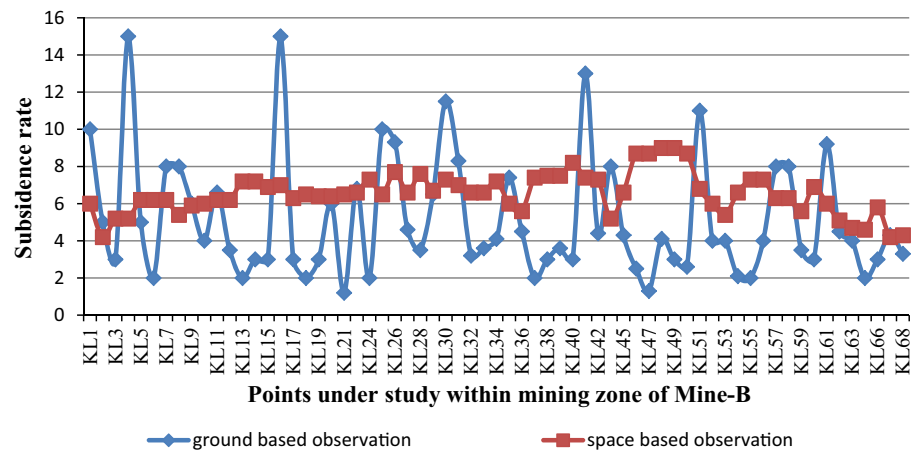


**Fig. 8** Comparison of results obtained from space based observation and ground based observation of all the points sections wise (Transverse sections)

**Fig. 9** Comparison of results obtained from space based observation and ground based observation of all the points in mining zone of Mine-B



problems related to conventional and advanced DInSAR technique for the study area.

**Funding** Indian Institute of Technology (Indian School of Mines), Dhanbad, India (FRS(89)/2014-15/ME).

## References

- Amelung, F., Galloway, D. L., Bell, J. W., Zebker, H. A., & Laczniak, R. J. (1999). Sensing the ups and downs of Las Vegas: InSAR reveals structural control of land subsidence and aquifer-system deformation. *Geology*, 27(6), 483–486.
- Amelung, F., Jonsson, S., Zebker, H., & Segall, P. (2000). Widespread uplift and ‘trapdoor’ faulting on Galapagos volcanoes observed with radar interferometry. *Nature*, 407, 993–996.
- Berardino, P., Fornaro, G., Lanari, R., & Sansosti, E. (2002). A new algorithm for surface deformation monitoring based on small baseline differential SAR interferograms. *IEEE TGRS*, 40(11), 2375–2383.
- Chatterjee, R. S. (2006). Subsidence in Kolkata (Calutta) City, India, during the 1990s as observed from space by differential synthetic aperture radar interferometry (D-InSAR) technique. *Remote Sensing of Environment*, 102, 176–185.
- Colesanti, C., Ferretti, A., Prati, C., & Rocca, F. (2002). Full exploitation of the ERS archive: Multi data set permanent scatterers analysis. In *Proceedings of the IEEE international geoscience and remote sensing symposium (IGARSS 2002)*, Vol. 2, Toronto (Canada), 24–28 June 2002, pp. 1234–1236.
- Colesanti, C., Ferretti, A., Prati, C., & Rocca, F. (2003). Monitoring landslides and tectonic motion with the permanent scatterers technique. *Engineering Geology*, 68(1–2), 3–14.
- Costantini, M., Falco, S., Malvarosa, F., & Minati, F. (2008). A new method for identification and analysis of persistent scatterers in series of SAR images. In *Proceedings of IGARSS 2008*, Boston.
- Crosetto, M., Biescas, E., Duro, J., Closa, J., & Arnaud, A. (2008). Quality assessment of advanced interferometric products based on time series of ERS and Envisat SAR data. *Photogrammetric Engineering and Remote Sensing*, 74(4), 443–450.
- Crosetto, M., Crippa, B., Biescas, E., Monserrat, O., Agudo, M., & Fernández, P. (2005). Land deformation monitoring using SAR interferometry: State-of-the-art. *Photogrammetrie Fernerkundung Geoinformation*, 6, 497–510.
- Devanathéry, N., Crosetto, M., Monserrat, O., Cuevas-González, M., & Crippa, B. (2014). An approach to persistent scatterer interferometry. *Remote Sensing*, 6(7), 6662–6679.
- Duro, J., Inglada, J., Closa, J., Adam, N., & Arnaud, A. (2003). High resolution differential interferometry using time series of ERS and ENVISAT SAR data. In *FRINGE 2003 workshop*, Vol. 550, p. 72.
- Ferretti, A., Fumagalli, A., Novali, F., Prati, C., Rocca, F., & Rucci, A. (2011). A new algorithm for processing interferometric data-stacks: SqueeSAR. *IEEE TGRS*, 49(9), 3460–3470.
- Ferretti, A., Prati, C., & Rocca, F. (2000). Nonlinear subsidence rate estimation using permanent scatterers in differential SAR interferometry. *IEEE TGRS*, 38(5), 2202–2212.
- Ferretti, A., Prati, C., & Rocca, F. (2001). Permanent scatterers in SAR interferometry. *IEEE TGRS*, 39(1), 8–20.
- Fruneau, B., & Sarti, F. (2000). Detection of ground subsidence in the city of Paris using radar interferometry: Isolation from atmospheric artefacts using correlation. *Geophysical Research Letters*, 27–24, 3981–3984.
- Gabriel, A. K., Goldstein, R. M., & Zebker, H. A. (1989). Mapping small elevation changes over large areas: differential radar interferometry. *Journal Geophysical Research*, 94, 9183–9191.
- Galloway, D. L., Hudnut, K. W., Ingebritsen, S. E., Phillips, S. P., Peltzer, G., Rogez, F., et al. (1998). Detection of aquifer system compaction and land subsidence using interferometric synthetic aperture radar, Antelope Valley, Mojave Desert, California. *Water Resources Research*, 34(10), 2573–2585.
- Goel, K., & Adam, N. (2014). A distributed scatterer interferometry approach for precision monitoring of known surface deformation phenomena. *IEEE TGRS*, 52(9), 5454–5468.
- Goldstein, R. (1995). Atmospheric limitations to repeat-track radar interferometry. *Geophysical Research Letters*, 22, 2517–2520.
- Hanssen, R. F. (2001). *Radar interferometry: Data interpretation and error analysis*. Dordrecht: Kluwer Academic Publishers.
- Hanssen, R., & Usai, S. (1997). Interferometric phase analysis for monitoring slow deformation processes. In *3rd ERS workshop (Florence)*. <http://florence97.ERS-symposium.org> 22, pp. 2517–2520.
- Hanssen, R., Weckwerth, T., Zebker, H., & Klees, R. (1999). High-resolution water vapor mapping from interferometric radar measurements. *Science*, 283(5406), 1297.
- Hetland, E. A., Musé, P., Simons, M., Lin, Y. N., Agram, P. S., & DiCapri, C. J. (2012). Multiscale InSAR time series (MInTS) analysis of surface deformation. *Journal of Geophysical Research: Solid Earth*. <https://doi.org/10.1029/2011JB008731>.
- Hooper, A. (2008). A multi-temporal InSAR method incorporating both persistent scatterer and small baseline approaches.



- Geophysical Research Letters*, 35, L16302. <https://doi.org/10.1029/2008GL034654>.
- Hooper, A., Zebker, H., Segall, P., & Kampes, B. (2004). A new method for measuring deformation on volcanoes and other natural terrains using InSAR persistent scatterers. *Geophysical Research Letters*. <https://doi.org/10.1029/2004GL021737>.
- Kampes, B. M. (2006). *Radar interferometry: Persistent scatterer technique*. Dordrecht: Springer.
- Lanari, R., Casu, F., Manzo, M., Zeni, G., Berardino, P., Manunta, M., et al. (2007). An overview of the small baseline subset algorithm: A DInSAR technique for surface deformation analysis. *Pure and Applied Geophysics*, 164(4), 637–661.
- López-Quiroz, P., Doin, M. P., Tupin, F., Briole, P., & Nicolas, J. M. (2009). Time series analysis of Mexico City subsidence constrained by radar interferometry. *Journal of Applied Geophysics*, 69(1), 1–15.
- Lv, X., Yazici, B., Zeghal, M., Bennett, V., & Abdoun, T. (2014). Joint-scatterer processing for time-series InSAR. *IEEE TGRS*, 52(11), 7205–7221.
- Massonnet, D., & Feigl, K. (1993). Satellite radar interferometric map of the coseismic deformation field of the M D 6:1 Eureka Valley California earthquake of May 17, 1993. *Geophysical Research Letters*, 22, 1541–1544.
- Massonnet, D., Vadon, H., & Rossi, M. (1996). Reduction of the need for phase unwrapping in radar interferometry. *IEEE Transactions on Geoscience and Remote Sensing*, 34, 489–497.
- Massonnet, D., Vadon, H., & Rossi, M. (1997). Reduction of the need for phase unwrapping in radar interferometry. *IEEE Transactions on Geoscience and Remote Sensing*, 34, 489–497.
- Mora, O., Mallorquí, J. J., & Broquetas, A. (2003). Linear and nonlinear terrain deformation maps from a reduced set of interferometric SAR images. *IEEE Transactions on Geoscience and Remote Sensing*, 41, 2243–2253.
- Perissin, D., & Wang, T. (2012). Repeat-pass SAR interferometry with partially coherent targets. *IEEE TGRS*, 50(1), 271–280.
- Raucoules, D., Bourguin, B., De Michele, M., Le Cozannet, G., Closset, L., Bremmer, C., et al. (2009). Validation and intercomparison of persistent scatterers interferometry: PSIC4 project results. *Journal of Applied Geophysics*, 68(3), 335–347.
- Rosen, P. A., Hensley, S., Zebker, H. A., Webb, F. H., & Fielding, E. J. (1996). Surface deformation and coherence measurements of Kilauea Volcano, Hawaii, from SIR-C radar interferometry. *Journal of Geophysical Researches*, 101(23109–23125), 1996.
- Schmidt, D., & Bürgmann, R. (2003). Time-dependent land uplift and subsidence in the Santa Clara valley, California, from a large interferometric synthetic aperture radar data set. *Journal of Geophysical Research*. <https://doi.org/10.1029/2002JB002267>.
- Strozzi, T., Dammert, P., Wegmüller, U., Martínez, J. M., Askne, J., Beaudoin, A., et al. (2001). Landuse mapping with ERS SAR interferometry. *IEEE Transactions on Geoscience and Remote Sensing*, 38(2), 766–775.
- Usai, S. (2001). A new approach for long term monitoring of deformations by differential SAR interferometry, Ph.D. thesis, Delft Univ. of Technol., Delft, The Netherlands. Williams.
- Van Leijen, F., & Hanssen, R. (2007). Ground water management and its consequences in Delft, the Netherlands as observed by persistent scatterer interferometry. In *Proceedings of FRINGE 2007*, Frascati (Italy).
- Werner, C., Wegmüller, U., Strozzi, T., & Wiesmann, A. (2003). Gamma SAR and interferometric processing software. In *Proceedings 16–20 October*, Gothernburg, Sweden.
- Zebker, H. A., & Goldstein, R. M. (1986). Topographic mapping from interferometric synthetic aperture radar observations. *Journal of Geophysical Research*, 91, 4993–4999.
- Zebker, H. A., & Rosen, P. (1994). On the derivation of coseismic displacement fields using differential radar interferometry: The Landers earthquake. In *International geoscience and remote sensing symposium IGARSS'94* (Pasadena, CA), pp. 286–288.